




**Blinking coupling enhances network synchronization**Fatemeh Parastesh,<sup>1</sup> Karthikeyan Rajagopal,<sup>2</sup> Sajad Jafari <sup>1,3</sup> Matjaž Perc <sup>4,5,6</sup> and Eckehard Schöll <sup>7,8,9,\*</sup><sup>1</sup>*Department of Biomedical Engineering, Amirkabir University of Technology (Tehran Polytechnic), Iran*<sup>2</sup>*Center for Nonlinear Systems, Chennai Institute of Technology, India*<sup>3</sup>*Health Technology Research Institute, Amirkabir University of Technology (Tehran Polytechnic), Iran*<sup>4</sup>*Faculty of Natural Sciences and Mathematics, University of Maribor, Koroška Cesta 160, 2000 Maribor, Slovenia*<sup>5</sup>*Department of Medical Research, China Medical University Hospital, China Medical University, Taichung 404332, Taiwan*<sup>6</sup>*Complexity Science Hub Vienna, Josefstädterstraße 39, 1080 Vienna, Austria*<sup>7</sup>*Institut für Theoretische Physik, Technische Universität Berlin, Hardenbergstrasse 36, D-10623 Berlin, Germany*<sup>8</sup>*Bernstein Center for Computational Neuroscience Berlin, Humboldt-Universität, D-10115 Berlin, Germany*<sup>9</sup>*Potsdam Institute for Climate Impact Research, Telegrafenberg A 31, D-14473 Potsdam, Germany*

(Received 17 November 2021; accepted 13 April 2022; published 5 May 2022)

This paper studies the synchronization of a network with linear diffusive coupling, which blinks between the variables periodically. The synchronization of the blinking network in the case of sufficiently fast blinking is analyzed by showing that the stability of the synchronous solution depends only on the averaged coupling and not on the instantaneous coupling. To illustrate the effect of the blinking period on the network synchronization, the Hindmarsh-Rose model is used as the dynamics of nodes. The synchronization is investigated by considering constant single-variable coupling, averaged coupling, and blinking coupling through a linear stability analysis. It is observed that by decreasing the blinking period, the required coupling strength for synchrony is reduced. It equals that of the averaged coupling model times the number of variables. However, in the averaged coupling, all variables participate in the coupling, while in the blinking model only one variable is coupled at any time. Therefore, the blinking coupling leads to an enhanced synchronization in comparison with the single-variable coupling. Numerical simulations of the average synchronization error of the network confirm the results obtained from the linear stability analysis.

DOI: [10.1103/PhysRevE.105.054304](https://doi.org/10.1103/PhysRevE.105.054304)**I. INTRODUCTION**

Complex dynamical networks have attracted much attention in recent years [1]. A universal phenomenon in these networks is the synchronized behavior of the components [2–4]. It has been shown that the structure of the network plays a key role in synchronization [5]. For this reason, many studies were focused on the influence of the network topology on synchronization. Wang *et al.* [6] proposed that the synchronizability of a homogeneous network can be enhanced by considering weighted and asymmetric couplings, similar to a scale-free network. Nishikawa *et al.* [7] reported that networks with a homogeneous distribution of connectivity, although having larger average path lengths, are more likely to synchronize than those with heterogeneous connectivity.

Enhancing synchronization is of great importance in many applications, including diverse brain functions [8,9]. For example, synchronization is essential in many memory processes such as working memory and long-term memory by enhancing neural plasticity [10]. In the attention-related process, the neurons receiving the attended stimuli exhibit enhanced synchrony in the gamma band [11]. In contrast to these desirable functions, some of the pathological brain

states are caused by increased synchrony in special regions. For instance, in patients with Parkinson's disease, abnormal synchronization is observed in the cortico-basal ganglia circuits [12]. In the past years, many efforts have been devoted to enhancing synchrony in dynamic networks. Lin and Chen [13] demonstrated that two chaotic oscillators could become synchronous by applying white-noise-based coupling. It has been shown that assigning the direction to the links of a network, for example, by the residual degree gradient (RDG) method or the residual edge-betweenness gradient method [14,15] can improve the synchronization. Ramirez *et al.* [16] proposed a dynamic coupling for a master-slave network and showed the enhanced synchronization, which could not be obtained with static coupling. Banerjee *et al.* [17] found that applying a parameter mismatch to well-defined oscillators of the network, such that the identical oscillators interact indirectly, can help achieve synchronization. Sevilla-Escoboza *et al.* [18] investigated the stability of synchronization by considering multivariable couplings and extracted the optimal scheme that resulted in maximum stability. Panahi *et al.* [19] revealed that the optimal synchronization in circulant oscillators is obtained by multivariable coupling with equal coupling coefficients. Time delay is another factor impacting synchronization [20,21]. Kyrychko *et al.* [22] examined the stability of different types of synchronization in different topologies considering distributed time delays in coupling.

\*schoell@physik.tu-berlin.de

They considered uniform and gamma delay distributions and found that the stability of the synchronization is improved with increasing the width of a uniform distribution or decreasing the mean of the gamma distribution. Gjurchinovski *et al.* [23] studied a network of coupled limit-cycle oscillators with time-varying delays in the coupling and self-feedbacks. They analyzed the stability of synchronization and found that the time-varying delay leads to the formation of amplitude death. Liu *et al.* [24] considered a network with time-varying delay and investigated local and global exponential synchronization. By using the average dwell time method, delay-dependent sufficient conditions were derived.

In realistic networks, the interactions between components are dynamic and evolve in time [25]. The varying communications between individuals in society or the interactions between neurons in the brain are some examples. In this context, many researchers have focused on synchronization in time-varying networks in the last two decades. Belykh *et al.* [26] proposed a small-world network with fixed nonlocal connections and time-varying links between any pairs of oscillators with the chaotic attractor. The blinking connections were switched on and off with pre-defined probability. It was found that the addition of random links reduces the effective path length and also enhances synchronization with a lower cost. Hasler *et al.* [27] considered blinking random connections in non-neighboring nodes in a multistable network. They showed that for sufficiently small blinking periods, i.e., fast switching, the behavior of the blinking network and the time-averaged network is almost the same. A comparison of the fast switching network and its averaged network has also been performed for finite time and infinite time intervals considering different cases according to the invariance or noninvariance of the numbers of attractors of the averaged system [28,29]. Porfiri [30] established a method for finding necessary and sufficient conditions for the stochastic synchronization of a network of chaotic maps with blinking links. Lu *et al.* [31] analyzed the synchronization of discrete-time networks with time-varying topologies by using the Hajnal diameter, which is equivalent to transverse Lyapunov exponents. Besides blinking small-world networks, synchronization of time-varying random networks has also been considered. Jeter and Belykh [32] studied the global stability of the synchronization in networks with time-varying random topology and intrinsic parameters. In another study, they found an optimal window of frequency in which the synchronization is stable [33]. Barabash and Belykh [34] studied a random network with time-varying connections and showed its equivalence with the averaged network for fast blinking. They found that synchronization is maintained even when increasing the blinking period considerably. Furthermore, with an increasing number of oscillators in the network, the synchronization threshold becomes independent from the blinking period. The effect of memory in the blinking links has also been studied. Liu *et al.* [35] proposed a novel approach for deriving sufficient conditions for the synchronization of networks with time-varying coupling structure and weight. They considered two cases for stochastic switching processes where in the first case, the sequences had an independent and identical random distribution and in the second case, the sequences created a Markov chain. Porfiri and Belykh [36] investigated two

one-dimensional coupled nonlinear maps under Markovian switching with respect to memory effects. Lanza *et al.* [37] analyzed synchronization in coupled memristor-based oscillatory circuits since memristors have represented a crucial function in the emergence of synchronization in special cases [38]. They showed the effects of blinking links on the invariant manifolds of oscillators.

In the studies mentioned above, the topologies of the networks were considered to be time varying with fixed coupling functions. However, there exists another configuration where the network connections between the nodes are fixed, but the coupling function is a time-varying function. The coupling function determines which dynamic variables of different nodes are connected with each other, i.e., it determines how the interactions among two (or more) dynamical systems evolve [39]. There are many applications in which the coupling function is time varying such as the cardiorespiratory system, transport grids and supply networks, and neural cross-frequency coupling functions [40,41]. In general, a coupling function is defined by its strength and its form. Some previous studies have focused on networks with time-varying coupling strength [42–44], while some have investigated the effects of time-varying coupling forms [39,45–47]. For example, Hagos *et al.* [45] reported synchronization transitions induced by time-varying coupling functions in phase oscillators. They indicated that the collective behavior of the oscillators depends on the shape of the coupling function, and the net coupling strength has a negligible effect. As an application in machine learning, Stelzer *et al.* [47] discussed deep neural networks with steplike switching functions between multiple time-delayed feedbacks to achieve a better, more efficient performance. These virtual networks consist of a single node with multiple time-delayed feedback loops.

In this paper, we consider a network with fixed connections and a special time-varying coupling function. The variable through which the oscillators are coupled is assumed to alternate between the system's variables periodically. Thus, the coupling function turns out to be blinking. The synchronization of the network is analyzed under fast blinking. The Hindmarsh-Rose neuron model is considered as the dynamics of each node of the network. The synchronization stability is investigated by computing the largest Lyapunov exponent of the variational equation for different blinking periods. It is found that by decreasing the blinking period, synchronization is achieved for lower coupling strengths. Numerical simulations are also performed, and the average synchronization error is calculated.

## II. THE BLINKING NETWORK MODEL

A time-varying dynamical network composed of  $N$  identical oscillators with linear diffusive coupling is considered. It is assumed that the links are constant, but the variable used in the coupling is switched periodically in time. Thus, the network can be described by

$$\dot{X}_i = F(X_i) + \sigma \sum_{j=1}^N G_{ij} H(t) X_j, \quad i = 1, \dots, N, \quad (1)$$

where  $X_i = (x_{i1}, x_{i2}, \dots, x_{id})$  is the  $d$ -dimensional state variable of the oscillators,  $F(X_i) : \mathbb{R}^d \rightarrow \mathbb{R}^d$  is the system's dynamics, and  $\sigma$  is the coupling strength. The network topology is determined by the adjacency matrix  $G_{N \times N}$  with zero row sum (i.e., the negative of the Laplacian matrix), where  $G_{ij} = 1$  if the  $i$ th and  $j$ th oscillators are connected and  $G_{ij} = 0$  else, and  $G_{ii} = -\sum_{j=1, j \neq i}^N G_{ij}$ . The time-varying matrix  $H(t) : \mathbb{R}^d \rightarrow \mathbb{R}^d$  is the internal-coupling matrix and determines which variables are considered in the coupling at each time  $t$ . Here, the matrix  $H(t)$  is assumed to blink between variables with equal time intervals with period  $\tau$ . Therefore, the matrix  $H(t)$  and its elements  $H_{mn}(t)$  ( $m, n = 1, \dots, d$ ) can be described as follows:

$$\begin{aligned} H_{mm}(t) &= \begin{cases} 1 & \text{if } \frac{(m-1)\tau}{d} < t < \frac{m\tau}{d}, \\ 0 & \text{otherwise} \end{cases}, \\ H_{mn}(t) &= 0, \\ H(t + \tau) &= H(t). \end{aligned} \quad (2)$$

This time-varying network can have a synchronous solution  $s(t) = X_i(t)$ ,  $i = 1, \dots, N$ . The stability of the synchronous manifold is equivalent to the stability of the error vector  $\eta_i(t) = X_i(t) - s(t)$  with respect to perturbations around zero. Substituting  $\eta_i(t)$  into the network equation [Eq. (1)], one obtains the linearized variational equation,

$$\dot{\eta}_i(t) = DF_s(t)\eta_i(t) + \sigma \sum_{j=1}^N G_{ij} DH_s(t)\eta_j(t), \quad (3)$$

where  $DF_s : \mathbb{R}^d \rightarrow \mathbb{R}^d$  and  $DH_s : \mathbb{R}^d \rightarrow \mathbb{R}^d$  are the Jacobian matrices of  $F$  and  $H$  at  $s(t)$ . Note that since the coupling is considered to be linear diffusion, we have  $DH_s(t) = H(t)$ . Thus, the system of linearized coupled oscillators is given in terms of the  $Nd$ -dimensional vector  $\eta(t) = (\eta_1, \eta_2, \dots, \eta_N)$  by

$$\dot{\eta}(t) = (I_N \otimes DF_s(t) + \sigma(G \otimes H(t)))\eta(t), \quad (4)$$

where  $\otimes$  is the Kronecker product. The matrix  $G$  can be diagonalized using Schur decomposition. Therefore, an upper triangular matrix is formed with eigenvalues of  $G$  appearing on its main diagonal. Finally, diagonalizing  $G$ , and since the first term of Eq. (4) is block diagonal, the set of variational equations [Eq. (4)] can be transformed to the decoupled system,

$$\dot{\eta}(t) = [DF_s(t) + \sigma \lambda_k H(t)]\eta(t), \quad k = 1, \dots, N, \quad (5)$$

where  $\lambda_k$  are the eigenvalues of the adjacency matrix ( $G$ ) and  $\eta(t)$  is a  $d$ -dimensional vector. For a network with a connected graph, the first eigenvalue is always zero, and thus, the system [Eq. (5)] for  $k = 1$  evolves along the synchronous manifold. Consequently, the stability of the system [Eq. (5)] needs to be checked for  $k = 2, \dots, N$ , which corresponds to the directions transverse to the synchronous manifold. This method is called the master stability approach and has been proposed by Pecora and Carroll [5]. The master stability function (MSF) is defined as the largest Lyapunov exponent ( $\Lambda$ ) of the variational Eq. (5) as a function of the complex parameter  $\mu = \lambda_k$ . If  $\Lambda(\mu) < 0$  for all eigenvalues  $\mu = \lambda_k$ ,  $k = 2, \dots, N$ , the synchronized solution is stable. Huang *et al.* [48] systematically studied the typical behavior of the MSF with different coupling schemes

for some well-known chaotic systems and categorized the MSF behavior into four classes.

### III. SYNCHRONIZATION UNDER FAST BLINKING

The stability of synchronization of the time-varying network with a sufficiently fast blinking coupling function can be estimated by the synchronization of the averaged network. Stilwell *et al.* [49] proved this theory for the network with time-varying topology. Here, we use the same approach for the time-varying coupling function. In this regard, the following theorem is given.

*Theorem 1.* It is supposed that the system of oscillators with linear diffusive coupling and the static internal coupling function ( $\bar{H}$ ) as

$$\dot{X}_i = F(X_i) + \sigma \sum_{j=1}^N G_{ij} \bar{H} X_j, \quad i = 1, \dots, N \quad (6)$$

has a stable synchronization manifold. Then, there exists a small  $\varepsilon^*$ , such that the set of oscillators with time-varying internal coupling function as

$$\dot{X}_i = F(X_i) + \sigma \sum_{j=1}^N G_{ij} H(t/\varepsilon) X_j, \quad i = 1, \dots, N \quad (7)$$

reaches a stable synchronization manifold for  $0 < \varepsilon < \varepsilon^*$ , if

$$\frac{1}{\tau} \int_t^{t+\tau} H(\alpha) d\alpha = \bar{H}. \quad (8)$$

The above theorem can be easily proved according to the following lemma, which is given for the fast switching systems.

*Lemma 1.* Supposing  $\dot{x}(t) = (A(t) + \bar{E})x(t)$  has a uniformly exponentially stable solution, where  $E$  is a matrix function satisfying  $\bar{E} = \frac{1}{\tau} \int_t^{t+\tau} E(\alpha) d\alpha$  for all  $t$ . Then, there exists small  $\varepsilon^*$  such that for  $0 < \varepsilon < \varepsilon^*$ ,  $\dot{z}(t) = (A(t) + E(t/\varepsilon))z(t)$  has a uniformly exponentially stable solution.

The proof of the lemma is presented in the Appendix [49].

*Proof of Theorem 1.* In the previous section, it was described that the stability of synchronization of the network [Eq. (6)] is equivalent to the stability of the linearized variational equation,

$$\dot{\eta} = [DF_s + \sigma \lambda_k \bar{H}]\eta, \quad k = 2, \dots, N. \quad (9)$$

Supposing that the network (6) achieves synchronization, then the system (9) is exponentially stable. According to the internal coupling matrix defined in the previous section and Eq. (2), there exists an average matrix,  $\bar{H} =$

$$\frac{1}{\tau} \int_t^{t+\tau} H(\alpha) d\alpha = \begin{bmatrix} 1/d & 0 & \dots & 0 \\ 0 & 1/d & \ddots & 0 \\ \vdots & \ddots & \ddots & 0 \\ 0 & \dots & 0 & 1/d \end{bmatrix}, \quad \text{for all } t. \quad \text{Thus,}$$

according to the lemma, there is  $\varepsilon^*$  such that the following system is exponentially stable,

$$\dot{\eta} = [DF_s + \sigma \lambda_k H(t/\varepsilon)]\eta, \quad k = 2, \dots, N. \quad (10)$$

The system (10) can be considered as the linearized variational equation of the network (7). Therefore, the time-varying network [Eq. (7)] can achieve stable synchronization.

From this theory, it can be concluded that when the blinking of the internal coupling function is sufficiently fast, i.e., the period of blinking is considerably smaller than the period of the oscillators, the stability of synchronization of the blinking network is determined by the synchronization stability of the averaged network. Therefore, the synchronization stability is not dependent on the coupling function  $H(t)$  at time  $t$  but on the average of  $H(t)$ .

**IV. BLINKING NEURONAL NETWORK**

It has been shown that the interactions in the brain are not static and evolve in time [50–54]. The synaptic connections and also the strength of the connections change temporally to optimize the functionality of the neurons [55]. Since the focus of our studies is the blinking coupling function and not the network topology, we use a very simple network consisting of two nodes in order to gain insight into the mechanism of blinking coupling. Therefore, as an illustration of blinking coupling, we choose a well-known dynamic model from neuroscience, and investigate synchronization in a simple network of two coupled Hindmarsh-Rose neurons where the dynamics of each node ( $F(X)$ ) is described by

$$\begin{aligned} \dot{x}_1 &= x_2 + 3x_1^2 - x_1^3 - x_3 + I_{\text{ext}}, \\ \dot{x}_2 &= 1 - 5x_1^2 - x_2, \\ \dot{x}_3 &= r(s(x_1 + 1.6) - x_3), \end{aligned} \tag{11}$$

where  $x_1$ ,  $x_2$ , and  $x_3$  denote the membrane potential, the fast and slow recovery variables. The parameters are set to  $I_{\text{ext}} = 3.2$ ,  $r = 0.006$ ,  $s = 4$ , where each node exhibits chaotic bursting. The time series of the Hindmarsh-Rose model with these parameters is shown in Fig. 1(a). In our simplest example, the network is assumed to be composed of two nodes via  $G = \begin{bmatrix} -1 & 1 \\ 1 & -1 \end{bmatrix}$  with eigenvalues  $\lambda_1 = 0$  and  $\lambda_2 = -2$ . The synchronizability of the network is obtained by linear stability analysis and numerical simulations considering different cases for the internal coupling function as (a) constant coupling function on each state variable, (b) averaged coupling function ( $\bar{H}$ ), (c) blinking coupling function as Eq. (2). It is notable that the synchronous manifold in all cases is also chaotic. An example of the time series of the synchronous neurons is illustrated in Fig. 1(b).

**A. Linear stability analysis**

At first, the coupling function is considered to be constant, with the coupling in one variable only. In this case, the stability of synchronization can be obtained by finding the stability of the variational equation [Eq. (5)] with constant  $H$  with respect to the zero solution. If the master stability function, defined as the largest Lyapunov exponent ( $\Lambda$ ) of the variational Eq. (5) as a function of the complex parameter  $\mu$ , satisfies  $\Lambda(\mu) < 0$  for all eigenvalues  $\mu = \lambda_k$  of the adjacency matrix, the synchronized solution is stable. For the considered coupling matrix  $G = \begin{bmatrix} -1 & 1 \\ 1 & -1 \end{bmatrix}$  with eigenvalues  $\lambda_1 = 0$  and  $\lambda_2 = -2$ , we have to compute the largest Lyapunov exponent ( $\Lambda$ ) of the variational equation for  $\mu = \lambda_2 = -2$ .

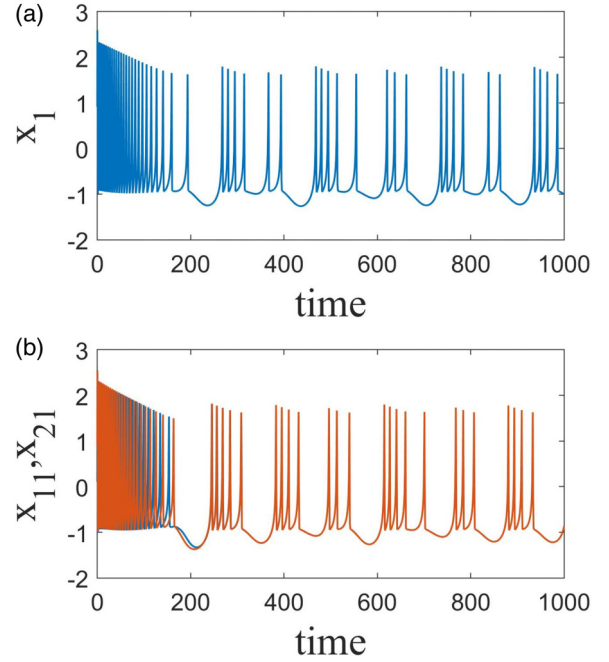


FIG. 1. (a) Time series of the membrane potential  $x_1$  of the single Hindmarsh-Rose neuron model [Eq. (11)] that exhibits chaotic bursting. The parameters are set to  $I_{\text{ext}} = 3.2$ ,  $r = 0.006$ ,  $s = 4$ . (b) Synchronous time series of two neurons coupled through  $x_1$  variables and coupling strength  $\sigma = 1$ . The blue and red colors represent the time series of the membrane potential of the first and second neurons  $x_{11}$  and  $x_{21}$ , respectively. The parameters are as in (a).

Figure 2 shows the largest Lyapunov exponent  $\Lambda(\mu = -2)$  for constant  $H$  as a function of the coupling strength. In Fig. 2(a), the coupling of the oscillators is through the  $x_1$  variables, i.e.,  $H = \begin{bmatrix} 1 & 0 & 0 \\ 0 & 0 & 0 \\ 0 & 0 & 0 \end{bmatrix}$ . With this coupling, synchronization can be attained for  $\sigma > 0.465$ . Figure 2(b) represents  $\Lambda(\mu = -2)$  for coupling in the  $x_2$  variables, i.e.,  $H = \begin{bmatrix} 0 & 0 & 0 \\ 0 & 1 & 0 \\ 0 & 0 & 0 \end{bmatrix}$ . It is observed that for this coupling, the network becomes synchronous for  $\sigma > 0.056$ . Finally, the coupling is through the  $x_3$  variables [Fig. 2(c)], i.e.,  $H = \begin{bmatrix} 0 & 0 & 0 \\ 0 & 0 & 0 \\ 0 & 0 & 1 \end{bmatrix}$ . In this case, the synchronization is unstable for any value of  $\sigma$ . Next,  $H = \begin{bmatrix} 1/3 & 0 & 0 \\ 0 & 1/3 & 0 \\ 0 & 0 & 1/3 \end{bmatrix}$  is considered, which is the average of the blinking network. The largest Lyapunov exponent, which is illustrated in Fig. 2(d), shows that the synchronization of the averaged network is achieved for  $\sigma > 0.021$ . It can be clearly seen that the largest Lyapunov exponent is a decreasing linear function of the coupling strength  $\sigma$ , which follows from the diagonal coupling in all three variables [56,57], in contrast to the coupling in only one variable in Figs. 2(a)–2(c). The stability of the synchronized solution  $\eta = 0$  is governed by the linearized equation  $\dot{\eta} = [DF_s + \lambda_2 \sigma I/3]\eta$

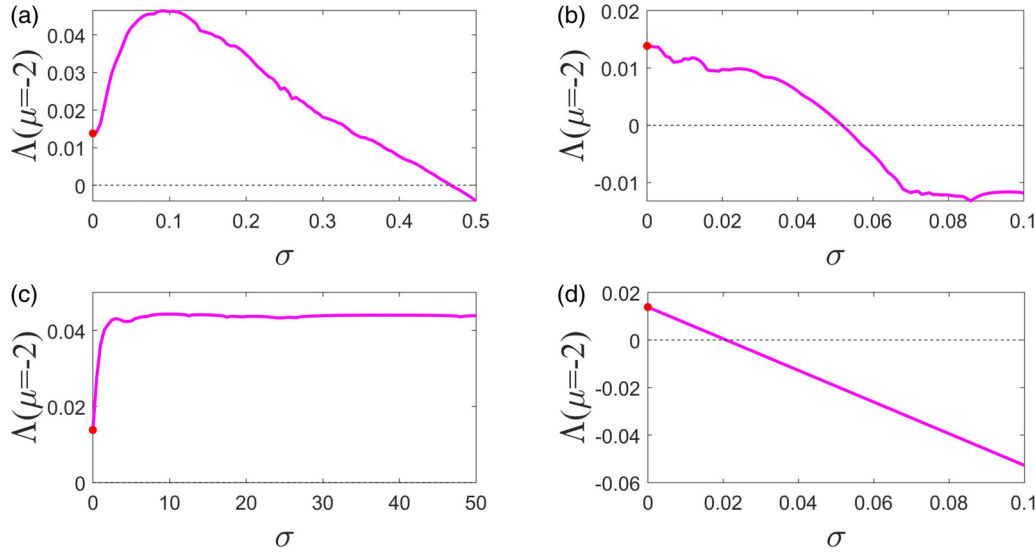


FIG. 2. The largest Lyapunov exponent  $\Lambda$  of the variational Eq. (5) for  $\mu = -2$  with constant coupling function ( $H$ ) in dependence on the coupling strength  $\sigma$ . (a) Coupling in  $x_1$  variables, (b) coupling in  $x_2$  variables, (c) coupling in  $x_3$  variables, (d) averaged network. Parameters as in Fig. 1.

with  $\lambda_2 = -2$  for perturbations of  $\eta = 0$ , where  $I$  is the unity matrix. In fact, for a constant matrix  $A_0 = DF_s$  the eigenvalues  $\gamma_0$  of  $A_0$  are related to the eigenvalues  $\gamma$  of  $A = [DF_s + \lambda_2\sigma I/3]$  by  $\gamma = \gamma_0 + \lambda_2\sigma/3$  which follows from comparing the two eigenvalue equations. Since the Lyapunov exponents correspond to the real part of the eigenvalues averaged along the attractor's orbits, the eigenvalue equation  $\gamma = \gamma_0 + \lambda_2\sigma/3$  can be converted to the equation  $\Lambda = \Lambda_0 + \lambda_2\sigma/3$ , where  $\Lambda_0$  is the maximum Lyapunov exponent of  $DF_s$ . Therefore, the maximum Lyapunov exponent  $\Lambda$  as a function of  $\sigma$  is given by a straight line  $\Lambda = \Lambda_0 - 2\sigma/3$ . Consequently, the threshold for synchronization  $\Lambda = 0$  can be calculated as  $\sigma = 3\Lambda_0/2$  which gives  $\sigma = 0.0207$  for  $\Lambda_0 = 0.0138$ .

Next, we investigate the stability of the synchronous solution of the blinking network. The largest Lyapunov exponent of Eq. (5) is calculated for the time-varying coupling function, i.e.,

$$H(t) = \begin{cases} \begin{bmatrix} 1 & 0 & 0 \\ 0 & 0 & 0 \\ 0 & 0 & 0 \end{bmatrix} & \text{if } 0 < t < \tau/3 \\ \begin{bmatrix} 0 & 0 & 0 \\ 0 & 1 & 0 \\ 0 & 0 & 0 \end{bmatrix} & \text{if } \tau/3 < t < 2\tau/3, \\ \begin{bmatrix} 0 & 0 & 0 \\ 0 & 0 & 0 \\ 0 & 0 & 1 \end{bmatrix} & \text{if } 2\tau/3 < t < \tau \end{cases}$$

$$H(t + \tau) = H(t). \tag{12}$$

Figure 3 shows  $\Lambda(\mu = -2)$  for different blinking periods  $\tau$  as a function of the coupling strength  $\sigma$ . Although the coupling function is discontinuous in time, the linear stability analysis is straight forward since the coupling is linear. The master stability function has been extended to nonsmooth (discontinuous) nonlinear coupling in [58]. The

time scale of the spikes in the chaotic bursting oscillations of the single Hindmarsh-Rose model is approximately equal to  $T = 30$ . We have chosen the periods of blinking as  $\tau = T, T/5, T/10, T/100, T/1000, T/10000 = 30, 6, 3, 0.3, 0.03, 0.003$ . The time step for solving the equations is set at  $dt = 0.0002$ . It can be seen that as the blinking occurs faster (with decreasing the period of blinking  $\tau$ ), the threshold of the coupling strength at which the synchronization is achieved is decreased. Furthermore, when the blinking period decreases sufficiently, i.e., for  $\tau < 0.03$ , synchronization can be obtained for  $\sigma > 0.021$ . For fast blinking the stability is the same as for the averaged coupling, and hence the maximum Lyapunov exponent decreases linearly with coupling strength as in Fig. 2 d. One can see that the function becomes more and more like a straight line with decreasing blinking period  $\tau$ . For the smallest value of  $\tau$

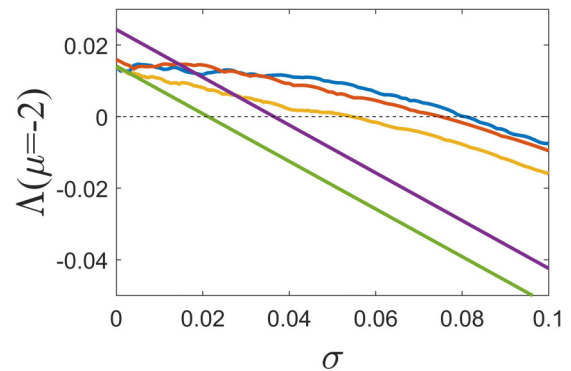


FIG. 3. The largest Lyapunov exponent ( $\Lambda(\mu = -2)$ ) of Eq. (3) vs the coupling strength ( $\sigma$ ) for different blinking periods  $\tau$ . (Blue)  $\tau = T = 30$ , (red)  $\tau = T/5 = 6$ , (orange)  $\tau = T/10 = 3$ , (purple)  $\tau = T/100 = 0.3$ , (green)  $\tau = T/1000 = 0.03$ . For faster blinking, the largest Lyapunov exponent is the same as the green line with threshold  $\sigma = 0.021$ . Other parameters as in Fig. 1.

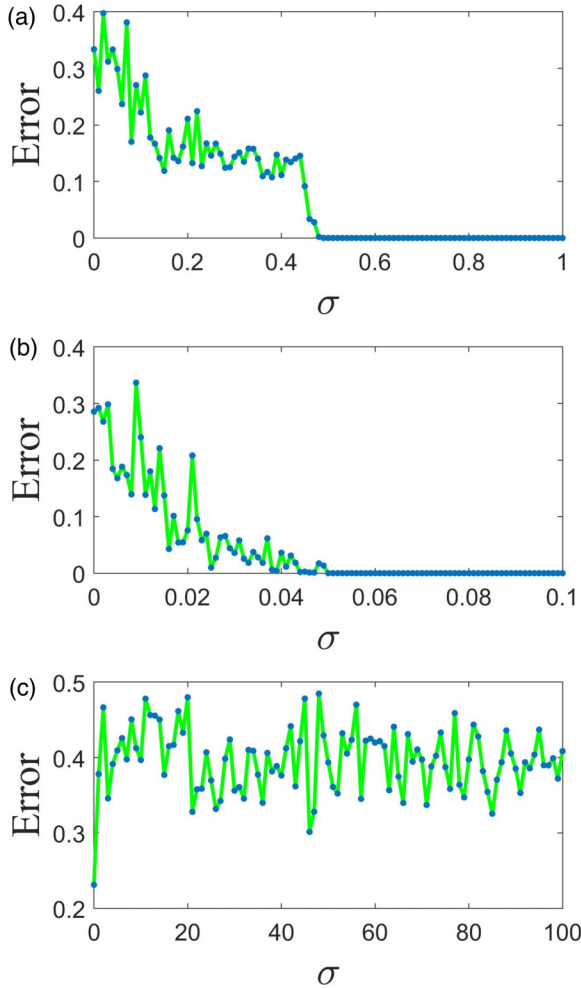


FIG. 4. The synchronization error vs the coupling strength  $\sigma$  with a constant coupling in (a)  $x_1$  variables, (b)  $x_2$  variables, (c)  $x_3$  variables. Parameters as in Fig. 1.

(green line) the graph becomes identical to Fig. 2(d), with the same critical coupling strength.

**B. Numerical results**

We have also solved the network dynamics of two coupled Hindmarsh-Rose neurons numerically. To evaluate the synchronization between two neurons, the temporally averaged synchronization error [59] is computed as

$$\text{Error} = \langle \|X_1(t) - X_2(t)\| \rangle_t, \tag{13}$$

where  $\langle \cdot \rangle_t$  denotes the time average. At first, the coupling is assumed to be constant through one of the variables. The synchronization error for the  $x_1$ -variable coupling is shown in Fig. 4(a). It can be seen that the neurons are synchronized for  $\sigma > 0.48$ . When the coupling is only in the  $x_2$  variables, the neurons become synchronous for  $\sigma > 0.05$ . The synchronization error for this coupling is shown in Fig. 4(b). Finally, when the neurons are coupled through the  $x_3$  variables, synchronization is not achieved at all by increasing the coupling strength [Fig. 4(c)]. Comparing Figs. 2 and 4 shows that the critical coupling strengths found by the numerical solution are

almost the same as those obtained from the linear stability analysis.

Now it is assumed that the coupling blinks between the three variables. Therefore, in the interval  $0 < \tau < \tau/3$ , the coupling is in the  $x_1$  variables, in  $\tau/3 < t < 2\tau/3$ , the coupling is in the  $x_2$  variables, and in  $2\tau/3 < t < \tau$ , the coupling is in the  $x_3$  variables. The synchronization errors for various blinking periods as in Fig. 3 are shown in Fig. 5. It is observed that when the period of blinking is long, the synchronization threshold is large. With decreasing blinking period  $\tau$ , synchronization is achieved for smaller coupling strengths, such that for  $\tau = 0.03$  the synchronization is stable approximately for  $\sigma > 0.02$ . The numerically found thresholds for stable synchronization are consistent with the results derived from the linear stability analysis.

To obtain an overview of the effect of the blinking period on the synchronization threshold, the parameter plane is presented in Fig. 6. The blinking period is considered to vary in the range  $\tau \in [0.01, 30]$  in a logarithmic scale to represent the short periods better. The values of the largest Lyapunov exponent of the linearized system [Eq. (5)] for  $\mu = -2$  are shown in Fig. 6(a). The black curve in this figure marks  $\Lambda = 0$  and separates the regions of asynchronous and synchronous behavior. Figure 6(b) represents the numerically obtained synchronization error [Eq. (13)] of the network. Note the nonmonotonic behavior of the synchronization threshold as a function of  $\tau$  which is visible both in Figs. 6(a) and 6(b).

**V. CONCLUSIONS**

In this paper, the synchronization of a time-varying network with blinking coupling variables was investigated. It was assumed that the links of the network are fixed and time independent, but the variable that participates in the coupling switches between the system’s variables with a well-defined periodicity. For the case of fast blinking, a theorem was presented which shows that the synchronization of the network under fast blinking is equivalent to the synchronization of the averaged network. Therefore, the instantaneous coupling configuration does not affect the synchrony of the network. Thus, in general, the blinking coupling function can enhance synchronization of systems in which the coupling strength needed for synchronization in single-variable coupling is higher than that for averaged diagonal coupling. This is a significant result and can be applied for enhancing the synchronization of any physical systems such as chaotic electronic circuits in which the coupling in all variables can be readily implemented [18], if those systems satisfy the above condition.

As an illustration, the Hindmarsh-Rose model was used to describe the dynamics of the nodes. At first, the synchronization of the network with constant coupling was studied by calculating the master stability function. It was observed that the best case for synchronization is the coupling through the  $x_2$  variables, which provides synchrony for  $\sigma > 0.056$ , but synchronization is never achieved for coupling in the  $x_3$  variables. Then, the necessary conditions for the stability of the synchronization of the blinking network were obtained for different blinking periods. It was found that a smaller period of switching leads the network towards syn-

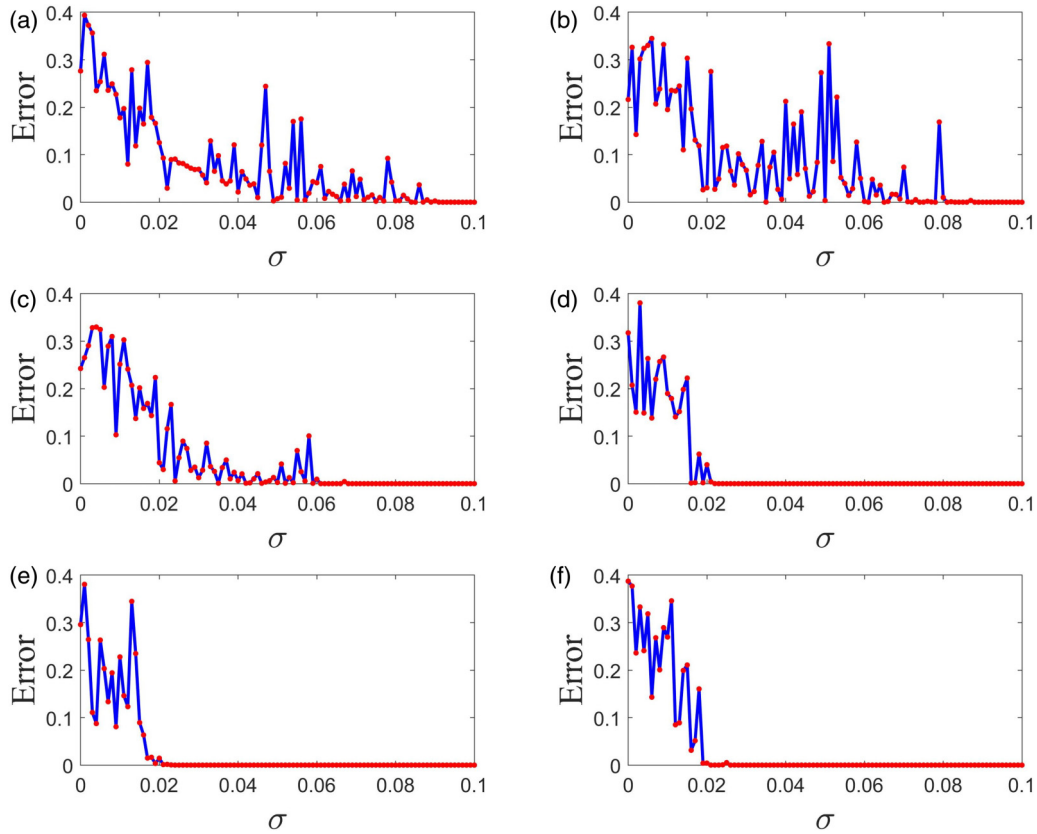


FIG. 5. The synchronization error vs coupling strength  $\sigma$  with blinking coupling for different blinking periods  $\tau$ . (a)  $\tau = T = 30$ , (b)  $\tau = T/5 = 6$ , (c)  $\tau = T/10 = 3$ , (d)  $\tau = T/100 = 0.3$ , (e)  $\tau = T/1000 = 0.03$ , (f)  $\tau = T/10\,000 = 0.003$ . Other parameters as in Fig. 1.

chronization at smaller coupling strengths. For sufficiently fast blinking, the blinking network with coupling strength  $\sigma$  is dynamically equivalent to fixed all-variable diagonal coupling with coupling strength  $\sigma/3$ , and the coupling strength needed for synchrony is considerably smaller than that needed in constant single-variable coupling, namely  $\sigma > 0.021$ . It is intriguing that the blinking coupling provides a better synchronization for the systems, although being periodically coupled in the  $x_3$  variable, which as a stand-alone coupling cannot lead to synchronization. The network was also studied

numerically, and the time-averaged synchronization error was computed. The numerical results agreed well with the conditions found from the linear stability approach.

ACKNOWLEDGMENTS

E.S. acknowledges support from Deutsche Forschungsgemeinschaft (DFG) Projects No. 429685422 and No. 440145547. M.P. is supported by the Slovenian Research Agency (Grants No. P1-0403 and No. J1-2457).

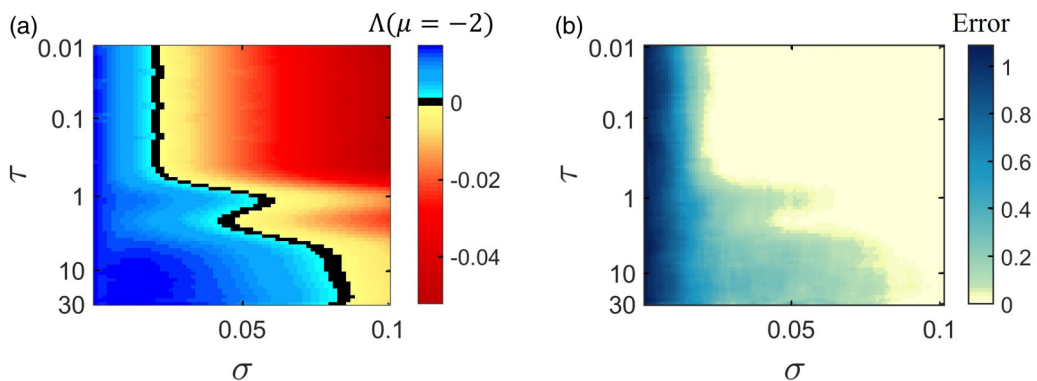


FIG. 6. The region of stable synchronization in the parameter plane of coupling strength  $\sigma$  and blinking period  $\tau$ . (a) The largest Lyapunov exponent of the linearized system [Eq. (5)] for  $\mu = -2$ ; the asynchronous and synchronous states' regions are separated by the black curve ( $\Lambda = 0$ ). (b) Numerically calculated synchronization error. Parameters as in Fig. 1.

**APPENDIX: PROOF OF LEMMA 1**

Here, the proof of Lemma 1 is presented [49].

In this lemma, it is supposed that the system  $\dot{x}(t) = (A(t) + \bar{E})x(t)$  is uniformly exponentially stable. Therefore, there exists a Lyapunov function  $v(x(t), t) = x^T(t)Q(t)x(t)$  with symmetric matrix  $Q(t)$  such that

$$\eta \|x(t)\|^2 \leq v(x(t), t) \leq \rho \|x(t)\|^2, \quad (\text{A1})$$

and

$$\frac{d}{dt}v(x(t), t) \leq -\mu \|x(t)\|^2, \quad (\text{A2})$$

where  $\eta > 0$ ,  $\rho > 0$ , and  $\mu > 0$ .

To prove the exponential stability of  $\dot{z}(t) = (A(t) + E(t/\varepsilon))z(t)$ , it is shown that  $v(z(t), t)$  is its Lyapunov function and the following equation is negative definite.

$$\Delta v(z(t + \varepsilon T), t) \equiv v(z(t + \varepsilon T, t + \varepsilon T) - v(z(t), t)). \quad (\text{A3})$$

Equation (A3) can be expanded to

$$\begin{aligned} \Delta v(z(t + \varepsilon T), t) &= z^T(t + \varepsilon T)Q(t + \varepsilon T)z(t + \varepsilon T) \\ &\quad - z^T(t)Q(t)z(t) = z^T(t)(\Phi_E^T(t + \varepsilon T, t)Q(t + \varepsilon T) \\ &\quad \times \Phi_E(t + \varepsilon T, t) - Q(t))z(t), \end{aligned} \quad (\text{A4})$$

where  $\Phi_E(t, \tau)$  denotes the transition matrix of  $A(t) + E(t/\varepsilon)$ . Then,  $H(t + \varepsilon T, t) = \Phi_E(t + \varepsilon T, t) - \Phi_{\bar{E}}(t + \varepsilon T, t)$  is defined, where  $\Phi_{\bar{E}}(t + \varepsilon T, t)$  denotes the transition matrix of  $A(t) + \bar{E}$ ,

$$\begin{aligned} H(t + \varepsilon T, t) &= \Phi(t + \varepsilon T, t) - \Phi_{\bar{E}}(t + \varepsilon T, t) \\ &= I + \int_t^{t+\varepsilon T} A(\sigma_1) + E\left(\frac{\sigma}{\varepsilon}\right) d\sigma \\ &\quad + \sum_{i=2}^{\infty} \int_t^{t+\varepsilon T} A(\sigma_1) + E\left(\frac{\sigma_1}{\varepsilon}\right) \int_t^{\sigma_1} \\ &\quad \times \dots \int_t^{\sigma_{i-1}} A(\sigma_i) + E\left(\frac{\sigma_i}{\varepsilon}\right) d\sigma_i \dots d\sigma_1 \\ &\quad - I - \int_t^{t+\varepsilon T} A(\sigma_1) + \bar{E} d\sigma \\ &\quad - \sum_{i=2}^{\infty} \int_t^{t+\varepsilon T} A(\sigma_1) + \bar{E} \int_t^{\sigma_1} \dots \int_t^{\sigma_{i-1}} A(\sigma_i) \\ &\quad + \bar{E} d\sigma_i \dots d\sigma_1. \end{aligned} \quad (\text{A5})$$

With considering

$$\int_t^{t+\varepsilon T} E\left(\frac{\sigma}{\varepsilon}\right) d\sigma = \varepsilon T \bar{E}, \quad (\text{A6})$$

Eq. (A5) turns into Eq. (A7),

$$\begin{aligned} H(t + \varepsilon T, t) &= \sum_{i=2}^{\infty} \int_t^{t+\varepsilon T} A(\sigma_1) + E\left(\frac{\sigma_1}{\varepsilon}\right) \\ &\quad \times \int_t^{\sigma_1} \dots \int_t^{\sigma_{i-1}} A(\sigma_i) + E\left(\frac{\sigma_i}{\varepsilon}\right) d\sigma_i \dots d\sigma_1 \\ &\quad - \sum_{i=2}^{\infty} \int_t^{t+\varepsilon T} A(\sigma_1) + \bar{E} \int_t^{\sigma_1} \end{aligned}$$

$$\times \dots \int_t^{\sigma_{i-1}} A(\sigma_i) + \bar{E} d\sigma_i \dots d\sigma_1. \quad (\text{A7})$$

Therefore, a bound for  $H(t + \varepsilon T, t)$  can be determined as

$$\|H(t + \varepsilon T)\| \leq 2(e^{\varepsilon T \alpha} - 1 - \varepsilon T \alpha), \quad (\text{A8})$$

where

$$\alpha \equiv \sup_{t \geq 0} (\max(\|A(t) + \bar{E}\|, \|A(t) + E(t/\varepsilon)\|)). \quad (\text{A9})$$

Substituting  $\Phi_E = \Phi_{\bar{E}} + H$  in Eq. (A4) yields

$$\begin{aligned} \Delta v(z(t + \varepsilon T), t) &= z^T(t)(\Phi_{\bar{E}}^T(t + \varepsilon T, t)Q(t + \varepsilon T) \\ &\quad \times \Phi_{\bar{E}}(t + \varepsilon T, t) - Q(t))z(t) + z^T(t) \\ &\quad \times (\Phi_E^T(t + \varepsilon T, t)Q(t + \varepsilon T) \\ &\quad \times H(t + \varepsilon T, t) + H^T(t + \varepsilon T, t) \\ &\quad \times Q(t + \varepsilon T)\Phi_E^T(t + \varepsilon T, t) + \\ &\quad \times H^T(t + \varepsilon T, t)Q(t + \varepsilon T) \\ &\quad \times H(t + \varepsilon T, t))z(t). \end{aligned} \quad (\text{A10})$$

To obtain an upper bound for  $\Delta v(z(t + \varepsilon T), t)$ , we should use some relationships which are derived from Eqs. (A1) and (A2), as

$$\|Q(t)\| \leq \rho, \quad (\text{A11})$$

$$\|\Phi_E^T(t, t_0)\| \leq \sqrt{\frac{\rho}{\eta}} e^{-\frac{\mu}{2\rho}(t-t_0)}, \quad (\text{A12})$$

$$v(x(t), t) \leq e^{-\frac{\mu}{2\rho}(t-t_0)} v(x(t_0), t_0), t \geq t_0. \quad (\text{A13})$$

The first term of Eq. (A10), with considering  $x(t) = z(t)$  as the initial condition, can be written as

$$\begin{aligned} z^T(t)(\Phi_{\bar{E}}^T(t + \varepsilon T, t)Q(t + \varepsilon T)\Phi_{\bar{E}}(t + \varepsilon T, t) \\ - Q(t))z(t) = v(x(t + \varepsilon T), t + \varepsilon T) - v(x(t), t), \end{aligned} \quad (\text{A14})$$

and, using Eqs. (A13) and (A1) yields

$$\begin{aligned} v(x(t + \varepsilon T), t + \varepsilon T) - v(x(t), t) \\ \leq (e^{-\frac{\mu \varepsilon T}{\rho}} - 1)v(x(t), t) \\ \leq \rho(e^{-\frac{\mu \varepsilon T}{\rho}} - 1)\|x(t)\|^2. \end{aligned} \quad (\text{A15})$$

Therefore,

$$\begin{aligned} z^T(t)(\Phi_E^T(t + \varepsilon T, t)Q(t + \varepsilon T)\Phi_E(t + \varepsilon T, t) \\ - Q(t))z(t) \leq \rho(e^{-\frac{\mu \varepsilon T}{\rho}} - 1)\|z(t)\|^2. \end{aligned} \quad (\text{A16})$$

With combining Eqs. (A8), (A11), (A12), and (A16), the upper bound can be obtained as

$$\begin{aligned} \Delta v(z(t + \varepsilon T), t) \\ \leq (\rho(e^{-\frac{\mu \varepsilon T}{\rho}} - 1) + 4\rho(\sqrt{\rho\eta}e^{-\frac{\mu \varepsilon T}{2\rho}})(e^{\varepsilon T \alpha} - 1 - \varepsilon T \alpha) \\ + 4\rho(e^{\varepsilon T \alpha} - 1 - \varepsilon T \alpha)^2)\|z(t)\|^2. \end{aligned} \quad (\text{A17})$$

By describing the right-hand side of (A17) by a continuously differentiable function  $g(\varepsilon, x)$ , we have  $g(0, z) = 0$ , and  $\frac{\partial}{\partial \varepsilon} g(0, z) = -\mu T \|z\|^2 \leq 0$ . Then, since for  $\varepsilon \rightarrow \infty$ ,



$g(\varepsilon, z) \rightarrow \infty$ , there is an  $\varepsilon^*$  such that for  $0 < \varepsilon < \varepsilon^*$  and  $z \neq 0$ ,  $g(\varepsilon^*, z) = 0$ , and  $g(\varepsilon, z) < 0$ . Therefore,  $\Delta v(z(t + \varepsilon T), t)$  is negative definite.

Now it is shown that the negative definiteness of  $\Delta v$  results in the stability of  $\dot{z}(t) = (A(t) + E(t/\varepsilon))z(t)$ .

With finding  $\varepsilon$  and  $\gamma > 0$  to satisfy

$$\begin{aligned} \Delta v(z(t_0 + \varepsilon T), t_0) &= v(z(t_0 + \varepsilon T), t_0 + \varepsilon T) - v(z(t_0), t_0) \\ &\leq -\gamma \|z(t_0)\|^2, \end{aligned} \quad (\text{A18})$$

and rewriting (A1) as  $v(z(t_0), t_0) \leq \rho \|z(t_0)\|^2$ , we obtain

$$v(z(t_0 + \varepsilon T), t_0 + \varepsilon T) - v(z(t_0), t_0) \leq -(\gamma/\rho)v(z(t_0), t_0), \quad (\text{A19})$$

or  $v(z(t_0 + \varepsilon T), t_0 + \varepsilon T) \leq (1 - \gamma/\rho)v(z(t_0), t_0)$  which yields  $v(z(t_0 + k\varepsilon T), t_0 + k\varepsilon T) \leq (1 - \gamma/\rho)^k v(z(t_0), t_0)$  for positive integer  $k$ .

Therefore, for  $k \rightarrow \infty$ ,  $v(z(t_0 + k\varepsilon T), t_0 + k\varepsilon T) \rightarrow 0$ , and then  $z(t_0 + k\varepsilon T) \rightarrow 0$ . Thus, the exponential stability of  $\dot{z}(t) = (A(t) + E(t/\varepsilon))z(t)$  is proved.

- 
- [1] S. Boccaletti, V. Latora, Y. Moreno, M. Chavez, and D.-U. Hwang, Complex networks: Structure and dynamics, *Phys. Rep.* **424**, 175 (2006).
- [2] A. Arenas, A. Díaz-Guilera, J. Kurths, Y. Moreno, and C. Zhou, Synchronization in complex networks, *Phys. Rep.* **469**, 93 (2008).
- [3] S. Boccaletti, A. N. Pisarchik, C. I. Del Genio, and A. Amann, *Synchronization: From Coupled Systems to Complex Networks* (Cambridge University Press, Cambridge, 2018).
- [4] R. Berner, *Patterns of Synchrony in Complex Networks of Adaptively Coupled Oscillators* (Springer Nature, Berlin/Heidelberg, 2021).
- [5] L. M. Pecora and T. L. Carroll, Master Stability Functions for Synchronized Coupled Systems, *Phys. Rev. Lett.* **80**, 2109 (1998).
- [6] X. Wang, Y.-C. Lai, and C. H. Lai, Enhancing synchronization based on complex gradient networks, *Phys. Rev. E* **75**, 056205 (2007).
- [7] T. Nishikawa, A. E. Motter, Y.-C. Lai, and F. C. Hoppensteadt, Heterogeneity in Oscillator Networks: Are Smaller Worlds Easier to Synchronize? *Phys. Rev. Lett.* **91**, 014101 (2003).
- [8] Y. Gong, B. Wang, and H. Xie, Spike-timing-dependent plasticity enhanced synchronization transitions induced by autapses in adaptive Newman-Watts neuronal networks, *Biosyst.* **150**, 132 (2016).
- [9] S. Rakshit, A. Ray, B. K. Bera, and D. Ghosh, Synchronization and firing patterns of coupled Rulkov neuronal map, *Nonlinear Dyn.* **94**, 785 (2018).
- [10] J. Fell and N. Axmacher, The role of phase synchronization in memory processes, *Nature Rev. Neurosci.* **12**, 105 (2011).
- [11] P. Fries, J. H. Reynolds, A. E. Rorie, and R. Desimone, Modulation of oscillatory neuronal synchronization by selective visual attention, *Science* **291**, 1560 (2001).
- [12] C. Hammond, H. Bergman, and P. Brown, Pathological synchronization in Parkinson's disease: Networks, models and treatments, *Trends Neurosci.* **30**, 357 (2007).
- [13] W. Lin and G. Chen, Using white noise to enhance synchronization of coupled chaotic systems, *Chaos* **16**, 013134 (2006).
- [14] A. Zeng, S.-W. Son, C. H. Yeung, Y. Fan, and Z. Di, Enhancing synchronization by directionality in complex networks, *Phys. Rev. E* **83**, 045101(R) (2011).
- [15] S.-W. Son, B. J. Kim, H. Hong, and H. Jeong, Dynamics and Directionality in Complex Networks, *Phys. Rev. Lett.* **103**, 228702 (2009).
- [16] J. P. Ramirez, A. Arellano-Delgado, and H. Nijmeijer, Enhancing master-slave synchronization: The effect of using a dynamic coupling, *Phys. Rev. E* **98**, 012208 (2018).
- [17] R. Banerjee, B. K. Bera, D. Ghosh, and S. K. Dana, Enhancing synchronization in chaotic oscillators by induced heterogeneity, *Eur. Phys. J. Spec. Top.* **226**, 1893 (2017).
- [18] R. Sevilla-Escoboza, R. Gutiérrez, G. Huerta-Cuellar, S. Boccaletti, J. Gómez-Gardeñes, A. Arenas, and J. M. Buldú, Enhancing the stability of the synchronization of multivariable coupled oscillators, *Phys. Rev. E* **92**, 032804 (2015).
- [19] S. Panahi, F. Nazarimehr, S. Jafari, J. C. Sprott, M. Perc, and R. Repnik, Optimal synchronization of circulant and non-circulant oscillators, *Appl. Math. Comput.* **394**, 125830 (2021).
- [20] E. Schöll, Synchronization in delay-coupled complex networks, in *Advances in Analysis and Control of Time-delayed Dynamical Systems* (World Scientific, Singapore, 2013), pp. 57–84.
- [21] J. Sawicki, *Delay Controlled Partial Synchronization in Complex Networks* (Springer Nature, Berlin/Heidelberg, 2019).
- [22] Y. Kyrychko, K. Blyuss, and E. Schöll, Synchronization of networks of oscillators with distributed delay coupling, *Chaos* **24**, 043117 (2014).
- [23] A. Gjurchinovski, A. Zakharova, and E. Schöll, Amplitude death in oscillator networks with variable-delay coupling, *Phys. Rev. E* **89**, 032915 (2014).
- [24] T. Liu, J. Zhao, and D. J. Hill, Exponential synchronization of complex delayed dynamical networks with switching topology, *IEEE Trans. Circuit. Syst. I* **57**, 2967 (2010).
- [25] S. Rakshit, S. Majhi, B. K. Bera, S. Sinha, and D. Ghosh, Time-varying multiplex network: Intralayer and interlayer synchronization, *Phys. Rev. E* **96**, 062308 (2017).
- [26] I. V. Belykh, V. N. Belykh, and M. Hasler, Blinking model and synchronization in small-world networks with a time-varying coupling, *Physica D* **195**, 188 (2004).
- [27] M. Hasler and I. Belykh, Blinking long-range connections increase the functionality of locally connected networks, *IEICE T. on Fund. Electr.* **88**, 2647 (2005).
- [28] M. Hasler, V. Belykh, and I. Belykh, Dynamics of stochastically blinking systems. Part I: Finite time properties, *SIAM J. Appl. Dyn. Syst.* **12**, 1007 (2013).
- [29] M. Hasler, V. Belykh, and I. Belykh, Dynamics of stochastically blinking systems. Part II: Asymptotic properties, *SIAM J. Appl. Dyn. Syst.* **12**, 1031 (2013).
- [30] M. Porfiri, Stochastic synchronization in blinking networks of chaotic maps, *Phys. Rev. E* **85**, 056114 (2012).

- [31] W. Lu, F. M. Atay, and J. Jost, Synchronization of discrete-time dynamical networks with time-varying couplings, *SIAM J. Math. Anal.* **39**, 1231 (2008).
- [32] R. Jeter and I. Belykh, Synchronization in on-off stochastic networks: Windows of opportunity, *IEEE Trans. Circuits Syst. I* **62**, 1260 (2015).
- [33] R. Jeter and I. Belykh, Dynamical networks with on-off stochastic connections: Beyond fast switching, in *Proceedings of the IEEE International Symposium on Circuits and Systems (ISCAS-2014)* (IEEE, New York, 2014), pp. 1788–1791.
- [34] N. Barabash and V. Belykh, Synchronization thresholds in an ensemble of Kuramoto phase oscillators with randomly blinking couplings, *Radiophys. Quantum El.* **60**, 761 (2018).
- [35] B. Liu, W. Lu, and T. Chen, Synchronization in complex networks with stochastically switching coupling structures, *IEEE Trans. Autom. Control* **57**, 754 (2012).
- [36] M. Porfiri and I. Belykh, Memory matters in synchronization of stochastically coupled maps, *SIAM J. Appl. Dyn. Syst.* **16**, 1372 (2017).
- [37] V. Lanza, J. Secco, and F. Corinto, Blinking networks of memristor oscillatory circuits in the flux-charge domain, *Front. Neurosci.* **15**, 618607 (2021).
- [38] A. Ascoli, V. Lanza, F. Corinto, and R. Tetzlaff, Synchronization conditions in simple memristor neural networks, *J. Franklin Inst.* **352**, 3196 (2015).
- [39] T. Stankovski, Time-varying coupling functions: Dynamical inference and cause of synchronization transitions, *Phys. Rev. E* **95**, 022206 (2017).
- [40] T. Stankovski, T. Pereira, P. V. E. McClintock, and A. Stefanovska, Coupling functions: Universal insights into dynamical interaction mechanisms, *Rev. Mod. Phys.* **89**, 045001 (2017).
- [41] B. Kralemann, M. Frühwirth, A. Pikovsky, M. Rosenblum, T. Kenner, J. Schaefer, and M. Moser, In vivo cardiac phase response curve elucidates human respiratory heart rate variability, *Nat. Commun.* **4**, 2418 (2013).
- [42] Z. Li, L. Jiao, and J.-J. Lee, Robust adaptive global synchronization of complex dynamical networks by adjusting time-varying coupling strength, *Physica A* **387**, 1369 (2008).
- [43] V. Chandrasekar, J. H. Sheeba, B. Subash, M. Lakshmanan, and J. Kurths, Adaptive coupling induced multi-stable states in complex networks, *Physica D* **267**, 36 (2014).
- [44] Q. Ren and J. Zhao, Adaptive coupling and enhanced synchronization in coupled phase oscillators, *Phys. Rev. E* **76**, 016207 (2007).
- [45] Z. Hagos, T. Stankovski, J. Newman, T. Pereira, P. V. E. McClintock, and A. Stefanovska, Synchronization transitions caused by time-varying coupling functions, *Philos. Trans. R. Soc. A* **377**, 20190275 (2019).
- [46] T. Stankovski, A. Duggento, P. V. E. McClintock, and A. Stefanovska, Inference of Time-Evolving Coupled Dynamical Systems in the Presence of Noise, *Phys. Rev. Lett.* **109**, 024101 (2012).
- [47] F. Stelzer, A. Röhm, R. Vicente, I. Fischer, and S. Yanchuk, Deep neural networks using a single neuron: Folded-in-time architecture using feedback-modulated delay loops, *Nat. Commun.* **12**, 1 (2021).
- [48] L. Huang, Q. Chen, Y.-C. Lai, and L. M. Pecora, Generic behavior of master-stability functions in coupled nonlinear dynamical systems, *Phys. Rev. E* **80**, 036204 (2009).
- [49] D. J. Stilwell, E. M. Bollt, and D. G. Roberson, Sufficient conditions for fast switching synchronization in time-varying network topologies, *SIAM J. Appl. Dyn. Syst.* **5**, 140 (2006).
- [50] S. Rakshit, B. K. Bera, D. Ghosh, and S. Sinha, Emergence of synchronization and regularity in firing patterns in time-varying neural hypernetworks, *Phys. Rev. E* **97**, 052304 (2018).
- [51] L. Zhang, Y. Wang, and Q. Wang, Synchronization for time-varying complex dynamical networks with different-dimensional nodes and non-dissipative coupling, *Commun. Nonlinear Sci. Numer. Simul.* **24**, 64 (2015).
- [52] S. Rakshit, S. Majhi, J. Kurths, and D. Ghosh, Neuronal synchronization in long-range time-varying networks, *Chaos* **31**, 073129 (2021).
- [53] S. Chakravartula, P. Indic, B. Sundaram, and T. Killingback, Emergence of local synchronization in neuronal networks with adaptive couplings, *PLoS One* **12**, e0178975 (2017).
- [54] D. Cumin and C. Unsworth, Generalising the Kuramoto model for the study of neuronal synchronisation in the brain, *Physica D* **226**, 181 (2007).
- [55] A. Destexhe and E. Marder, Plasticity in single neuron and circuit computations, *Nature (London)* **431**, 789 (2004).
- [56] A. Stefański, J. Wojewoda, T. Kapitaniak, and S. Yanchuk, Simple estimation of synchronization threshold in ensembles of diffusively coupled chaotic systems, *Phys. Rev. E* **70**, 026217 (2004).
- [57] A. Pikovsky, On the interaction of strange attractors, *Z Phys B: Condens Matter* **55**, 149 (1984).
- [58] J. Ladenbauer, J. Lehnert, H. Rankoohi, T. Dahms, E. Schöll, and K. Obermayer, Adaptation controls synchrony and cluster states of coupled threshold-model neurons, *Phys. Rev. E* **88**, 042713 (2013).
- [59] J. Sawicki, I. Omelchenko, A. Zakharova, and E. Schöll, Delay controls chimera relay synchronization in multiplex networks, *Phys. Rev. E* **98**, 062224 (2018).